J Nanostruct 15(3): 1303-1313, Summer 2025

RESEARCH PAPER

Characteristics of CdS Thin Film Nanoparticles Fabricated via Spray Pyrolysis Deposition

Mohammed Ahmed Mohammed

Department of Soil Sciences and Water Resources, College of Agriculture, University of Al-Qadisiyah, Al-Qadisiyah, Iraq

ARTICLE INFO

Article History:
Received 13 April 2025
Accepted 22 June 2025
Published 01 July 2025

Keywords:
CdS thin film
Gas sensor
Ohmic properties
Spray pyrolysis
Thin film nanoparticle

ABSTRACT

Spray pyrolysis was used to create nanocrystalline cadmium sulphide thin films on glass substrates in this study. Researcher looked examined how substrate temperature 400 °C affected the thin films' structural, morphological, optical, electrical, Photodetection Analysis, and NO_2 gas sensor characteristics. Analyses of the thin films' optical absorption, X-ray diffraction, and field emission scanning electron microscopy (FE-SEM) have been conducted. The thin films, according to the X-ray results, were polycrystalline and had a hexagonal phase crystallite. The thin films' surface is homogenous, consistent, and crack-free.The grains typically have an average size of 37.86 nm. The optical band gap values that have been found fall within the 2.4 eV range. Based on Hall effect testing, the thin films were found to have n-type conductivity. The generated CdS sheets were also used to create a photodetector, which worked admirably. A high photoresponsivity and external quantum efficiency were achieved using a 400 °C substrate temperature. At 40 ppm, the CdS film had a maximum reaction of 60% and was determined to be extremely sensitive to NO_2.

How to cite this article
Mohammed M. Characteristics of CdS Thin Film Nanoparticles Fabricated via Spray Pyrolysis Deposition. J Nanostruct, 2025; 15(3):1303-1313. DOI: 10.22052/JNS.2025.03.046

INTRODUCTION

Many new products, including sensors, have emerged in recent years based on CdS, proving that it is a technologically relevant material. For a while now, thin film cadmium sulphide solar cells have been touted as a potential replacement for the more common silicon devices. Several methods exist for depositing cadmium sulphide (CdS), such as elements evaporation [1], or co-evaporation [2], from a concentric cylinder source [3]. The authors [4], used a glass substrate to create an evaporated thin film. The rf diode sputtering method was used to produce CdS by [5]. The CdS film was sintered at 800°C after being screen-printed on alumina substrates by [6].

There has been significant interest in using II-VI chalcogenide compound semiconductors for optoelectronic and sensing applications [7-9]. Cadmium sulphide (CdS) possesses remarkable electrical and optical properties, rendering it a very suitable semiconductor for optoelectronic devices, distinguishing it from other II-VI semiconductors [10]. This is apparently characterized by a high rate of absorption in the visible region, has a large band gap of about 2.4 eV [11] and exhibits fast electron injection. Such possibilities as photodetectors and windows for heterojunction solar cells can be exploited in this

* *Corresponding Author Email: mohammed.ahmed@qu.edu.iq*

regard [12]. Photodetectors are very important optoelectronic devices used in medicine, military, communication and environmental sectors where optical detection is required [13]. For that reason it gets quite challenging to come up with such photodetectors which are cost effective as well as versatile enough to perform at various levels hence catering to different uses. This has led to an influx of materials used in photodetection hence extensive research on various materials and techniques employed in making these detectors. Materials like CdS are highly sought after when developing photodetectors that operate across wide range of wavelengths from UV to IR because they are wide-bandgap materials. These photodetectors find their applications in the areas of optical communications, sensing and imaging. The accuracy of this information is confirmed by reference [14]. Different methods have been reported for synthesis of cadmium sulfide (CdS) thin films including chemical bath deposition [15], electrodeposition [16], sputtering [17], spray pyrolysis [18]. Spray pyrolysis is a method that allows to produce films quickly and inexpensively over large areas. These films show both uniformity and strong adhesion to substrate [19]. This process involves dispersing a carefully prepared precursor solution into small droplets which are then deposited onto heated surfaces. At this point, the droplets decompose thermally creating an even coating on the surface with the desired molecule in it. There are various aspects through which quality of films produced during spraying can be controlled such as carrier gas pressure, flow rate and spray duration. Also, solution composition as well as temperature conditions also affects film quality [20]. The speed at which the solution flows is controlled by the gas pressure, which ultimately determines how evenly it spreads across a substrate; this has a great impact on the quality of the film. When we optimize spraying pressure, these films can be applied uniformly and smoothly to substrates. With respect to heterostructures formation intentional doping, layering or stacking is used in this context. The study included an investigation of the structural, optical and electrical properties for CdS thin films. The films were prepared over glass substrates at 400 °C, whilst the applied technique to deposition was spray pyrolysis. This included measurements that were done to assess the photo sensing character of materials and also establish whether no2 gas was present.

MATERIALS AND METHODS

In this case, thin film manufacturing of cadmium sulphide could be realized using a conventional spray pyrolysis technique with workforce participation [21]. A 0.2 M concentration of cadmium chloride and an identical amount ($(NH_2)_2CS$) thiourea are dissolved in distilled water for each substrate temperature to create a solution. The glass substrates were cleaned in ethanol before deposition and afterwards they were both dried for an additional time period in vacuum. As the foundations, slides under a microscope were used. The digital temperature controller was adjust to keep the substrate at 400 °C. To obtain thin films, approximately 5 mlmin of a sprayed ratio was utilized. The spray nozzle was separated from the glass substrate by 20 cm.

RESULT AND DISCUSSION

Structure Properties

Fig. 1 shows the XRD pattern of CdS thin Film obtained at substrate temperature 400°C. CdS thin Film nanoparticle have exhibited a polycrystalline structure. The lack of a defined structure in the glass substrate resulted in the wide peak observed in the XRD pattern depicted in Fig.1. The analysis of the study reveals that CdS can exhibit either a cubic or hexagonal crystal shape, or perhaps both, depending on the specific circumstances under which it is synthesised [22,23]. For solar cell applications, it is more advantageous to utilise thin films that possess a hexagonal structure [24].

Fig.1 reveal that CdS thin Film nanoparticle have a hexagonal shape characterised by the presence of (002), (102), (110), (103), (112),and (211) planes, as indicated by the JCPDS card number 89-0440 using (Jade- Programe xrd analysis). The XRD data indicate that the (002) plane has a favoured orientation in the film that is cultivated at a substrate temperature of 400°C, as reported by [25]. There is a noticeable preference for the (002) plane. This preference indicates that the atoms coming in are more likely to align themselves along this plane. It is worth mentioning that the wurtzite construction, which has the lowest surface energy, is associated with this plane [26]. When the substrate temperature 400 °C, the thermal energy and atomic fluctuations intensify, leading to a reduction in the density of nucleation centres. Consequently, a fewer number of centres initiate

growth. Consequently, a limited quantity of Cd and S atoms could adhere to the surface, resulting in a reduction in the crystallinity and thickness of the thin film.

The particle size of thin film was determined using the Scherrer Eq. 1:

$$D = 0.9\,\lambda / \beta \cos\theta \quad (1)$$

Where:

The variables in the equation are as follows: D represents the particle size, λ represents the X-ray wavelength (1.5406˚A), β represents the full width at half maximum (FWHM) in radians, and θ is the centre of the diffraction peak angle value, also in radians. The Full Width at Half Maximum (FWHM) value has been computed utilising the Jade-6 software.

The particle size calculated using Scherrer's equation is smaller than the actual sizes [27,28]. The broadening of peaks in XRD analysis is frequently attributed to technical variables and physical factors, including the dimensions of the crystallite and the strain within the lattice [29,30]. In terms of physical factors, the Full Width at Half Maximum (FWHM) of each diffraction peak can be mathematically represented as a linear combination of the effects caused by lattice strain and crystallite size, as determined by Scherrer's equation. When taking into account instrumental and strain broadenings, the true size

Table 1. lists the FWHM, d and D values for CdS thin film.

Peak No.	hkl	2ɵ deg	d A	B deg	D nm	Avg. D nm	lattice parameters		
1	(0 0 2)	26.659	3.34007	0.858	9.512377	37.86491	a	b	c
2	(1 0 2)	36.82	2.438312	0.56	14.94659		4.121	4.121	6.682
3	(1 1 0)	43.904	2.059906	0.924	9.266767				
4	(1 0 3)	48.115	1.888991	0.103	84.43816				
5	(1 1 2)	52.107	1.753267	0.781	11.31873				
6	(2 1 1)	71.261	1.321846	0.1	97.70681				

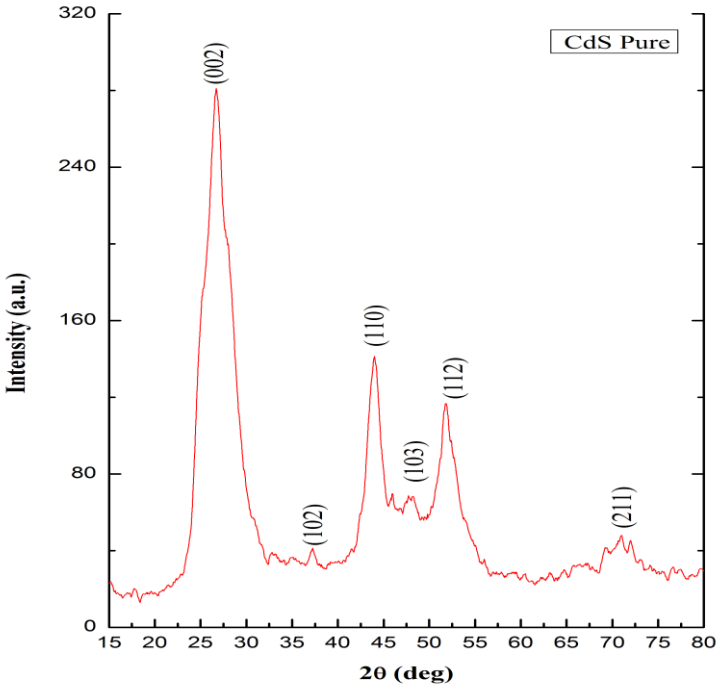

Fig. 1. XRD pattern of CdS thin Film nanoparticle at 400 °C.

of the crystallite will be slightly larger than the value obtained from measurement. The average particle diameter of the CdS thin Film nanoparticle measures 37.86 nm. The lattice parameters were determined utilizing Eq. 2.

$$\frac{1}{d^2} = \frac{3}{4}\left(\frac{d^2 + k + k^2}{a^2}\right) + \frac{t^1}{c^2} \quad (2)$$

The symbol d represents the distance between adjacent planes, while (h k l) denotes the Miller indices. The lattice constants are represented by the variables a and c. Table 1 provides the Full Width at Half Maximum (FWHM), d, and D values for the CdS thin film.

Fig. 2 displays three-dimensional atomic force microscopy (AFM) picture of CdS film, with dimensions of 4 µm × 4 µm. The films' surface exhibits topographical irregularities, characterised

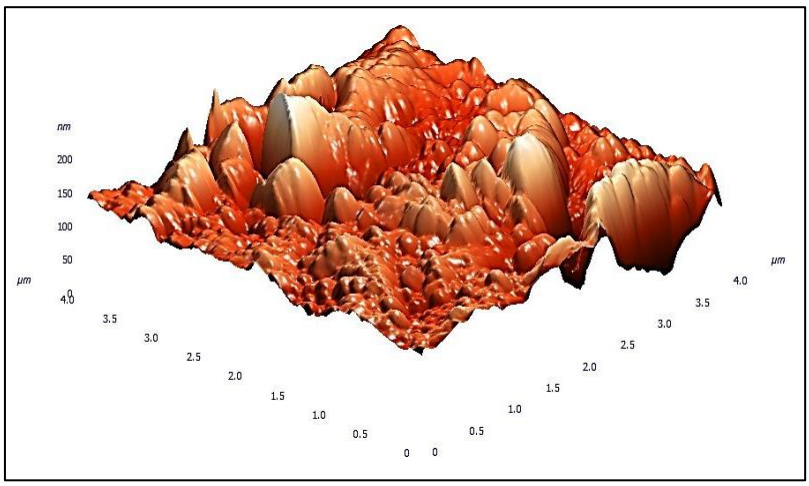

Fig. 2. AFM Image of CdS thin Film nanoparticle at 400 °C.

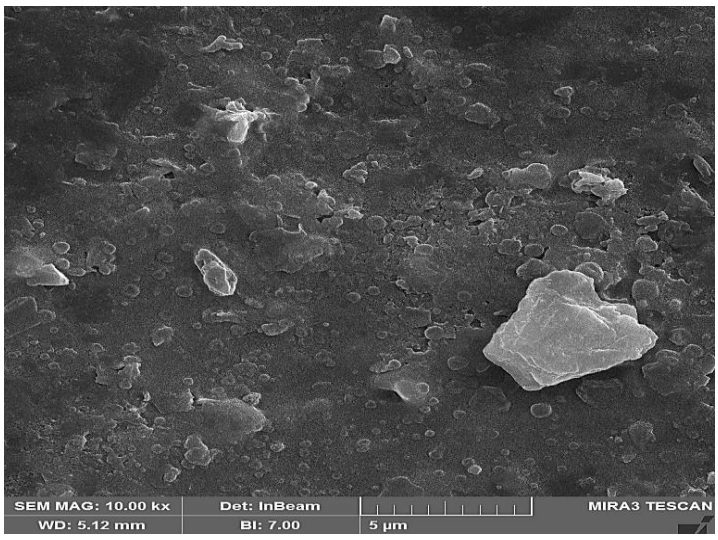

Fig. 3. FE-SEM image of CdS thin Film nanoparticle at 400 °C.

by peaks and valleys, which indicate its rough texture. The root mean square (RMS) of the film was 24.95 nm and Average Roughness was 17.44 nm.

The morphological features of the CdS thin Film nanoparticle are analyzed using the FE-SEM

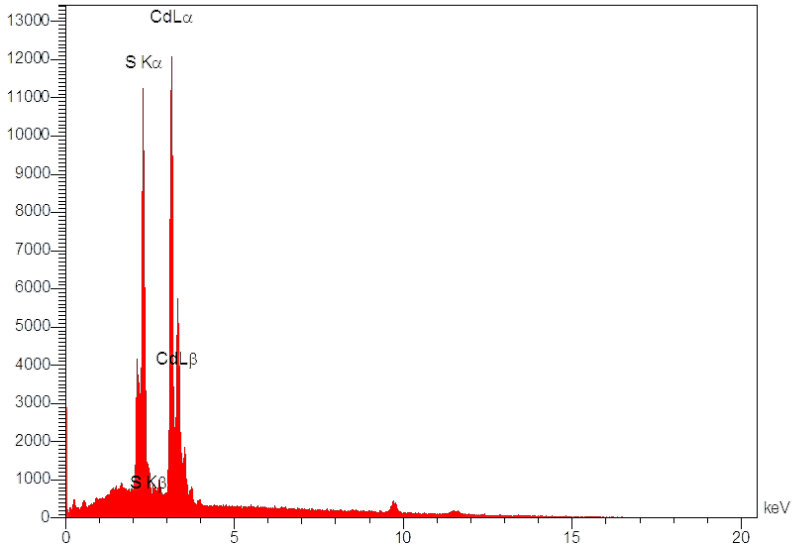

Fig. 4. EDAX analysis of CdS thin Film nanoparticle at 400 °C.

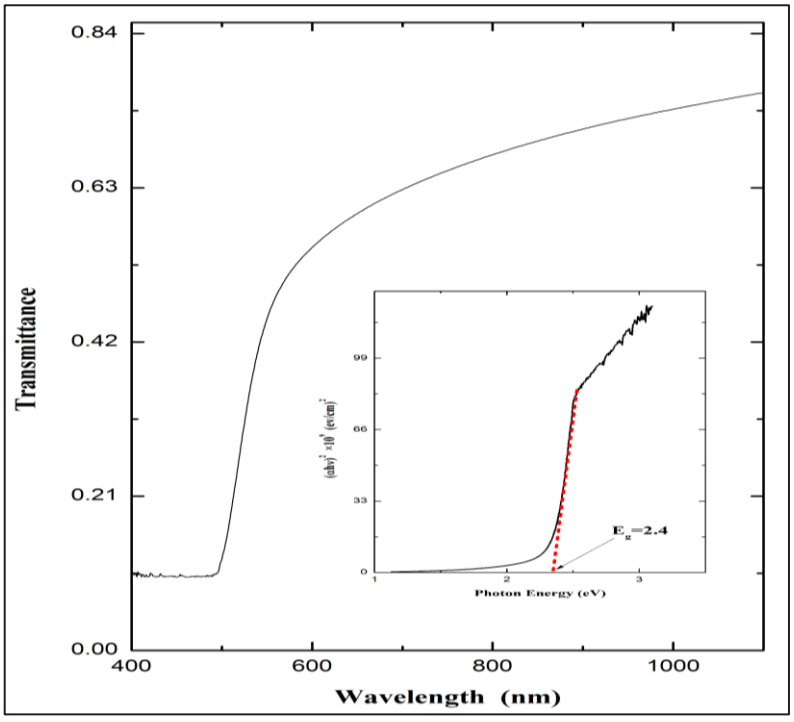

Fig. 5. Transmittance plot of CdS thin Film nanoparticle at 400°C.

image illustrated in Fig. 3. The thin film exhibits a uniform and smooth surface, devoid of any cracks or irregularities, and demonstrates a high degree of homogeneity. The mean grain size of the CdS thin film, fabricated at a substrate temperature of 400 °C, measures 49.78 nm.

The EDAX technology was employed to assess the elemental composition of a thin film. Fig. 4 depicts a standard EDAX spectrum of the CdS thin Film nanoparticle produced at a substrate temperature of 400°C. The identification of elemental peaks has confirmed the existence of cadmium and sulphur in the CdS thin film.

Optical Properties

In order to ascertain the optical properties of the spray-coated CdS thin Film nanoparticle within the wavelength range of 400–1100 nm, experiments were conducted to measure its optical transmittance. Fig. 5 displays the absorption spectra of the CdS thin Film nanoparticle coated at a subtract temperature of 400 oC, covering the ultraviolet, visible, and infrared ranges. The film exhibited the highest capacity for molecular absorption. The XRD and SEM tests indicate that the formation of uniform and polished grains is responsible for this phenomenon at the given temperature. In addition, the UV–Vis–IR absorption spectra show a steady movement of the edge-band which translated to change in bandgap due to temperature changes. The aim of this study was to calculate the bandgap energy for CdS thin Film nanoparticle and understand its characteristics. This was done by constructing Tauc plots, whereby the corresponding $(\alpha h\nu)^2$ is plotted over hν for each CdS film under study. The absorption coefficient (α) of the films was estimated using transmittance values and equation given by Eq. 3. The user's text is a mention of or reference to something.

$$\alpha h\nu = A(h\nu - Eg)^n \quad (3)$$

where T and t correspondingly denote the thickness of the film and the transmittance of the film, respectively.

For the purpose of obtaining the bandgap (E_g) values, the plot of $(\alpha h\nu)^2$ versus hν was produced based on the Tauc relation, which is represented by Eq. 4 [31]:

$$\alpha h\nu = A(h\nu - Eg)^n \quad (4)$$

When the photon energy is denoted by hν , the proportionality constant is denoted by A, and the number n is determined by the transition types.

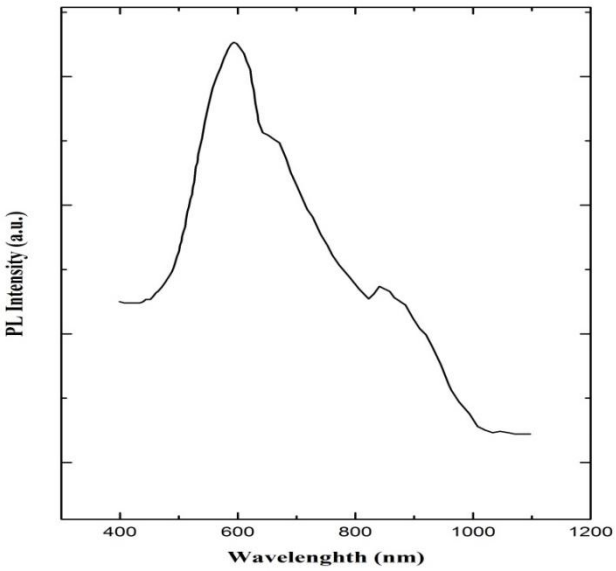

Fig. 6. Spectral analysis of the photoluminescence (PL) emitted by a thin film of (CdS) at a temperature of 400 °C.

The Tauc plot of the film that were deposited at 400 °C are displayed in the inset of Fig. 5.

The linear nature of the graphs indicates that the film possesses a direct bandgap. By extending the linear sections of the plots to the x-axis, it was possible to approximate the bandgaps of the film. The film's bandgap was determined to be 2.4 electron volts (eV).

PL Spectra

The film that was made at 400 °C also produced photoluminescence (PL) spectra. Fig. 6 shows the photoluminescence (PL) spectra) of the film taken at a 400 nm excitation wavelength; these spectra reveal the band-to-band transition emissions (a strong peak at 600 nm) and the defect-related emissions (a faint peak at 880 nm) [32]. With a little shift towards longer wavelengths, the CdS film that was coated at 400 °C shows the strongest band-to-band PL emission. In addition, the film's high quality is reinforced by the minimal intensity of the emission of defects (880 nm) generated by interstitial Cd or Cd vacancy defects.

Photodetection Analysis

The CdS photodetector, which was artificially produced, underwent testing to assess its ability to detect light in both the ultraviolet and visible spectrum. The I-V characteristics of the device, under both dark and 5 mW light-illuminated conditions, are depicted in Fig. 7. The device utilizes CdS film produced at a temperature of 400 °C. A schematic representation of the device is also included. The device's photocurrents were measured at potentials ranging from -5 V to +5 V, using 5 mW of UV and visible light. An increase in photocurrent relative to dark current indicates that the gadget has photosensing capabilities in the UV-Vis spectrum. The linear, symmetric I-V is a result of the film's Ohmic properties. The device's ON/OFF ratio, as measured by the picture and dark currents ratio, is 35. High current is seen in both dark and light circumstances in the device made utilising the film that was developed under 400 °C. The reduced resistivity of the film, as a result of its improved quality, is indicated by the reduction in dark current. An improvement in crystalline quality is suggested by this photocurrent rise.

In real-world settings, photodetectors' sensitivity is defined by their response and recovery times. The photodetector device's photo-switching responsiveness was measured during five ON/OFF cycles with a 5V constant bias and light levels adjusted manually in 1 mW increments. As shown in Fig. 8, the device's ON/OFF photo-switching response varies from 1 to 5 mW of light power. When seen in Fig. 8, the photocurrent grows in a straight line when the lamp power for

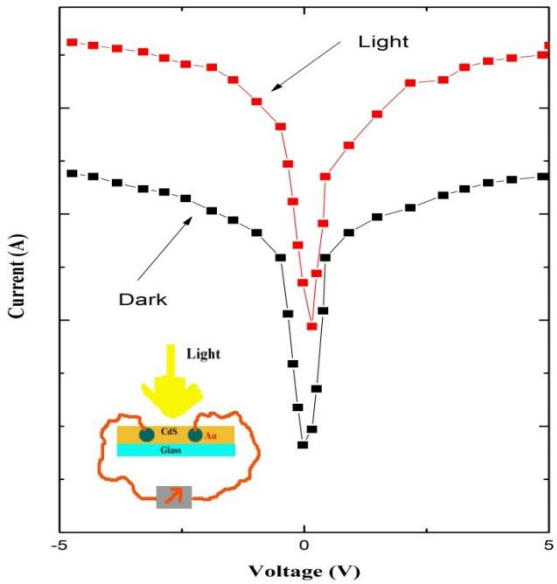

Fig. 7. I-V characteristics and photodetector schematic of CdS thin Film nanoparticle at 400 °C.

the device increases. This adds to the evidence of the device's outstanding photoresponse. The light power was gradually raised from 1 to 5 mW with each switching cycle. Because the film is very sensitive, increasing the light intensity causes the current to rise with each cycle.

The current in each cycle peaks at 0.2 s after the light is turned on. When the light is turned off, the current also drops quickly (0.5 s). The ON state experiences a tiny rise, whereas the OFF state experiences a tiny dip, as a result of differences in temperature. The manufactured photodetector is effective because of its high stability and reversibility.

In addition, the photodetector's external quantum efficiency, photoresponsivity, and

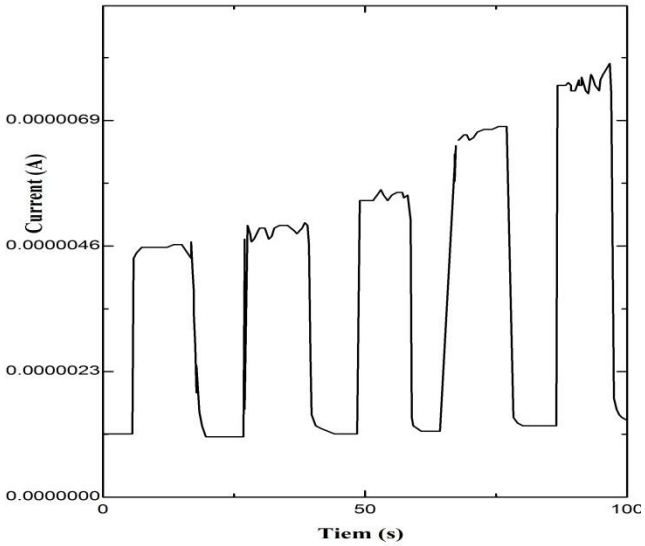

Fig. 8. CdS thin Film nanoparticle and their photo-switching properties at 400 °C.

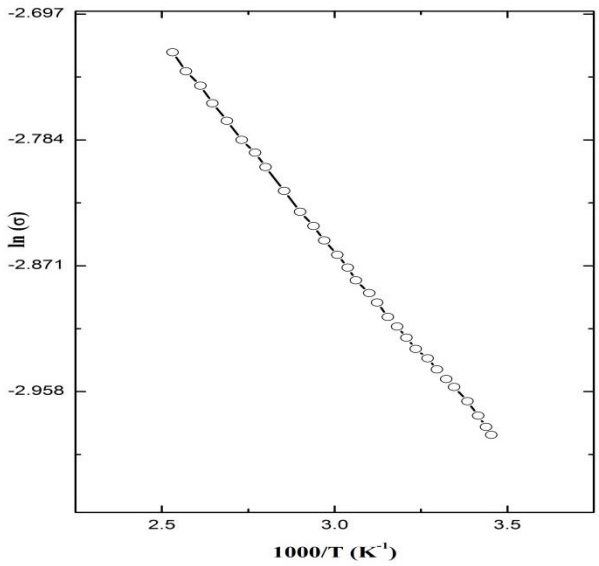

Fig. 9. Conductivity (σ) versus 1000/T characteristics for CdS thin Film nanoparticle at 400 °C.

detectivity were computed. The quantity of photocurrent created by light irradiation, or photoresponsivity (R), may be represented by Eq. 5 [33]:

$$R = \frac{I_p}{P_{in} \times A} \quad (5)$$

Ip represents the photocurrent created, which is equal to the difference between Iph (the photocurrent generated by incoming light) and Idark (the dark current). Pin represents the intensity of the incident light, and A represents the active area of the device. The particular detectivity (D*) of a photodetector may be calculated by utilising Eq. 6, which relates it to the responsivity.

$$D^* = R\sqrt{\frac{A}{2e\, I_{dark}}} \quad (6)$$

Eq. 7 may be used to determine the external quantum efficiency (EQE), which is the ratio of the number of incident photons to the number of electron-hole pairs created.

$$EQE = R\frac{h_c}{e\lambda} \quad (7)$$

Using the aforementioned equation, we were able to determine the several key parameters of the photodetector that were made using CdS film. The film that was made at 400 °C had a detectivity of 21×10^{10} Jones, an external quantum efficiency of 59.5%, and a responsivity of 17.6 AW^{-1}.

Electrical Properties

It was discovered that the CdS thin Film nanoparticle formed in the spray pyrolysis was almost stoichiometric. CdS has conductivity of the n-type. The Hall effect was used to measure the charge carriers' nature. Fig. 9 shows that the conductivity is 10^{-8} ohms cm^{-1}. Departures from the stiochiometry caused by sulphur vacancies or cadmium excesses can regulate conductivity.

Study CdS thin Film nanoparticle as NO_2 Gas Sensor

For examination of the CdS sensor's reaction to NO_2 gas. I tested the CdS sensor's sensitivity to several NO_2 gas concentrations in order to find its minimum detectable level. I have investigated the

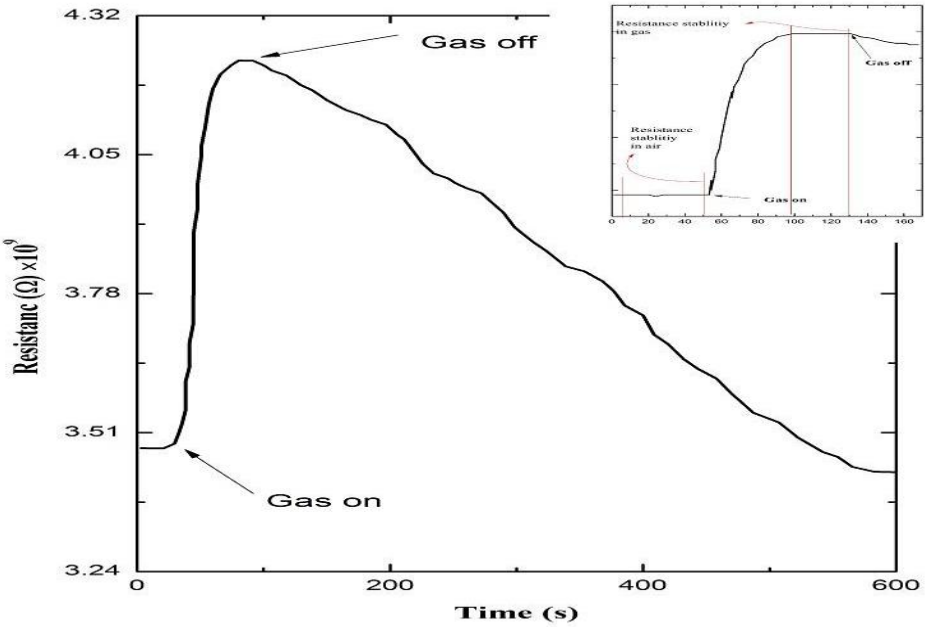

Fig. 10. Electrical response of CdS film with time for 40 ppm NO_2 gas (inset show NO_2 response stabilization).

NO2 gas detection capabilities of CdS sensors at values ranging of 40 ppm. The electrical response of CdS film to 40 ppm of NO_2 is shown in Fig. 10. After being exposed to NO_2 gas, the resistance increases significantly, reaches a steady value, and then progressively lowers when moved to clean air. The CdS films' porous nature, which causes surface phenomena to dominate over bulk material phenomena, might be the reason for the increase in resistance after exposure to NO_2. When the system reaches dynamic equilibrium, the resistance stabilizes.

CONCLUSION

This work created nanocrystalline cadmium sulphide thin coatings on glass substrates using spray pyrolysis. Researcher evaluated how substrate temperature 400 °C influenced thin films' structural, morphological, optical, electrical, Photodetection Analysis, and NO_2 gas sensor properties. Optical absorption, X-ray diffraction, and FE-SEM were used to analyse thin films. X-rays showed polycrystalline thin films with hexagonal crystallites. The thin films' surface is smooth and crack-free.The average particle size is 37.86 nm. Found optical band gaps are around 2.4 eV. Hall effect measurements showed n-type conductivity in thin sheets. CdS sheets were utilised to make a photodetector that performed well. A 400 °C substrate temperature produced strong photoresponsivity and external quantum efficiency. CdS film was particularly sensitive to NO_2 at 40 ppm, with a maximum response of 60%.

CONFLICT OF INTEREST

The authors declare that there is no conflict of interests regarding the publication of this manuscript.

REFERENCES

1. Raji P, Sanjeeviraja C, Ramachandran K. Thermal and structural properties of spray pyrolysed CdS thin film. Bull Mater Sci. 2005;28(3):233-238.
2. Burton LC, Hench TL. $Zn_xCd_{1-x}S$ films for use in heterojunction solar cells. Appl Phys Lett. 1976;29(9):612-614.
3. Burton LC, Baron B, Hench TL, Meakin JD. Formation and characterization of (CdZn)S films and (CdZn)S/Cu2s heterojunctions. J Electron Mater. 1978;7(1):159-171.
4. Raji P, Sanjeeviraja C, Ramachandran K. Thermal properties of nano crystalline CdS. Cryst Res Technol. 2004;39(7):617-622.
5. Fraser DB, Cook HD. Sputter deposition of Cd1−x Znx S photoconductive films. Journal of Vacuum Science and Technology. 1974;11(1):56-59.
6. Padam GK, Shanker V, Ghosh PK. Physical and electrical properties of screen-printed Zn_xCd_{1-x} thick films. Journal of Materials Science. 1988;23(3):1064-1067.
7. Shkir M, Ashraf IM, Chandekar KV, Yahia IS, Khan A, Algarni H, et al. A significant enhancement in visible-light photodetection properties of chemical spray pyrolysis fabricated CdS thin films by novel Eu doping concentrations. Sensors and Actuators A: Physical. 2020;301:111749.
8. Xu W, Liu H, Zhou D, Chen X, Ding N, Song H, et al. Localized surface plasmon resonances in self-doped copper chalcogenide binary nanocrystals and their emerging applications. Nano Today. 2020;33:100892.
9. Murugadoss G, Ramasamy V. Synthesis and optical characterization of single phased $ZnS:Mn^{2+}$/CdS core–shell nanoparticles. Spectrochimica Acta Part A: Molecular and Biomolecular Spectroscopy. 2012;93:70-74.
10. Murugadoss G, Thangamuthu R, Jayavel R, Rajesh Kumar M. Narrow with tunable optical band gap of CdS based core shell nanoparticles: Applications in pollutant degradation and solar cells. J Lumin. 2015;165:30-39.
11. Geng X, Zhang C, Debliquy M. Cadmium sulfide activated zinc oxide coatings deposited by liquid plasma spray for room temperature nitrogen dioxide detection under visible light illumination. Ceram Int. 2016;42(4):4845-4852.
12. Ismail RA, Al-Samarai A-ME, Ali AY. Preparation and characteristics study of CdS/macroporous silicon/c-Si double heterojunction photodetector by spray pyrolysis technique. Optik. 2018;168:302-312.
13. Zhao Y, Yuan M, Chen Y, Huang Y, Lian J, Cao S, et al. Size controllable preparation of sphere-based monolayer CdS thin films for white-light photodetectors. Ceram Int. 2018;44(2):2407-2412.
14. Pei Y, Pei R, Liang X, Wang Y, Liu L, Chen H, et al. CdS-Nanowires Flexible Photo-detector with Ag-Nanowires Electrode Based on Non-transfer Process. Sci Rep. 2016;6(1).
15. Waldiya M, Narasimman R, Bhagat D, Vankhade D, Mukhopadhyay I. Nanoparticulate CdS 2D array by chemical bath deposition: Characterization and optoelectronic study. Materials Chemistry and Physics. 2019;226:26-33.
16. Nobari N, Behboudnia M, Maleki R. Systematics in morphological, structural and optoelectrical properties of nanocrystalline CdS thin films grown by electrodeposition method. Materials Science and Engineering: B. 2017;224:181-189.
17. Das NK, Chakrabartty J, Farhad SFU, Sen Gupta AK, Ikball Ahamed EMK, Rahman KS, et al. Effect of substrate temperature on the properties of RF sputtered CdS thin films for solar cell applications. Results in Physics. 2020;17:103132.
18. Aksay S, Polat M, Özer T, Köse S, Gürbüz G. Investigations on structural, vibrational, morphological and optical properties of CdS and CdS/Co films by ultrasonic spray pyrolysis. Appl Surf Sci. 2011;257(23):10072-10077.
19. Al-Ani SKJ, Ismail RA, Al-Ta'ay HFA. Optoelectronic properties n:CdS:In/p-Si heterojunction photodetector. Journal of Materials Science: Materials in Electronics. 2006;17(10):819-824.
20. Paulraj K, Ramaswamy S, Yahia IS, Alshehri AM, Somaily HH, Kim H-S, et al. Praseodymium doped PbS thin films for optoelectronic applications prepared by nebulizer spray pyrolysis. Appl Phys A. 2020;126(7).
21. Idan MH, Kadhim RG, Mohammed MA. Preparation and study of the effect of adding cobalt and magnesium on the

morphological, optical properties and bacterial activity of cadmium sulfide compound. AIP Conference Proceedings: AIP Publishing; 2023. p. 040117.
22. Ikhmayies SJ, Juwhari HK, Ahmad-Bitar RN. Nanocrystalline CdS: In thin films prepared by the spray-pyrolysis technique. J Lumin. 2013;141:27-32.
23. He X-w, Liu W-f, Zhu C-f, Jiang G-s. CdS Thin Films Deposited by CBD Method on Glass. Chinese Journal of Chemical Physics. 2011;24(4):471-476.
24. Novruzov VD, Keskenler EF, Tomakin M, Kahraman S, Gorur O. Effects of ultraviolet light on B-doped CdS thin films prepared by spray pyrolysis method using perfume atomizer. Appl Surf Sci. 2013;280:318-324.
25. Hussein EH, Mohammed NJ, Al-Fouadi AHA, Abbas KN, Alikhan JS, Maksimova K, et al. Impact of deposition temperature on the structural properties of CdS/Si nanoparticles for nanoelectronics. Mater Lett. 2019;254:282-285.
26. Lee J. Raman scattering and photoluminescence analysis of B-doped CdS thin films. Thin Solid Films. 2004;451-452:170-174.
27. Medles M, Benramdane N, Bouzidi A, Nakrela A, Tabet-Derraz H, Kebbab Z, et al. Optical and electrical properties of Bi2S3 films deposited by spray pyrolysis. Thin Solid Films. 2006;497(1-2):58-64.
28. Madoun M, Baghdad R, Chebbah K, Bezzerrouk MA, Michez L, Benramdane N. Temperature effect on structural and optoelectronic properties of Bi2S3 nanocrystalline thin films deposited by spray pyrolysis method. Mater Sci Semicond Process. 2013;16(6):2084-2090.
29. Mageshwari K, Sathyamoorthy R. Nanocrystalline Bi2S3 thin films grown by thio-glycolic acid mediated successive ionic layer adsorption and reaction (SILAR) technique. Mater Sci Semicond Process. 2013;16(1):43-50.
30. Effect of antimony concentration on optical, electrical and structural properties of copper antimony sulphide thin films deposited by spray pyrolysis technique. Iranian Journal of Physics Research. 2022;22(3).
31. Alrababah YM, Sheng CK, Hassan MF. Influence of ammonium nitrate concentration on structural evolution and optical properties tuning of CdS nanoparticles synthesized by precipitation method. Nano-Structures and Nano-Objects. 2019;19:100344.
32. Gautam M, Shi Z, Jayatissa AH. Graphene films as transparent electrodes for photovoltaic devices based on cadmium sulfide thin films. Sol Energy Mater Sol Cells. 2017;163:1-8.
33. Amiri M, Alizadeh N. Highly photosensitive near infrared photodetector based on polypyrrole nanoparticle incorporated with CdS quantum dots. Mater Sci Semicond Process. 2020;111:104964.